Geology, Geophysics & Environment 2025, vol. 51 (2): 133–148

The combination of soil magnetometry with portable XRF spectroscopy as an effective tool for the assessment of sources of trace elements in topsoil

Tadeusz Magiera[1], Małgorzata Wawer-Liszka[2]

[1] *Institute of Environmental Engineering, Polish Academy of Sciences, Zabrze, Poland, ORCID ID: 0000-0002-8799-9421*
[2] *Institute of Environmental Engineering, Polish Academy of Sciences, Zabrze, Poland, e-mail: malgorzata.wawer@ipispan.edu.pl (corresponding author), ORCID ID: 0000-0001-9276-0880*

Received: 30 September 2024; accepted: 4 April 2025; first published online: 23 May 2025

Abstract: The origin of potentially toxic elements (PTEs) may influence their persistence, mobility and determine the extent to which they pose a threat to the soil environment. Therefore, the research objective of this study was to obtain information on the origin of nine PTEs present in the soil at two Natura 2000 protected areas. The second objective was to test the usability of three popular soil indices in assessing soil pollution in the study area. The research was carried out in two forested areas belonging to the Natura 2000 network of European protected areas, located in the Cieszyn region (southern Poland) on the Polish-Czech border. The research involved the analysis of the distribution of elements in topsoil cores (to 30 cm depth), based on high-resolution measurements obtained from a combination of soil magnetometry and portable XRF spectrometer (pXRF). Measurement of the vertical distribution of volume magnetic susceptibility (κ) along the core was performed using a Bartington MS2C sensor and the analysis of PTE contents using an Explorer 7000 XRF spectrometer. Based on the obtained results, three popular geochemical indices of soil contamination with metals and metalloids were calculated: geo-accumulation index (I_{geo}), single pollution index (*PI*), and enrichment index (*EF*).

Research has shown that the use of a pXRF spectrometer allows for the assessment of the distribution of PTEs in the soil profile with high accuracy, as well as a precise determination of the source of these elements and tracking the migration of pollutants deep into the soil profile. The peak of magnetic susceptibility values in the upper part of the profile strongly correlated with the contents of Pb, As and Zn, which confirmed the anthropogenic origin of these PTEs in the soil in both study areas. The distribution pattern of most of the remaining studied elements (Ti, V, Cr, Co, and Ni) in the soil profile and the analysis of geochemical indicators (I_{geo}, *PI* and *EF*) indicated their lithogenic and/or pedogenic origin.

The use of a pXRF spectrometer allows the assessment of the distribution of PTEs in the soil profile with high measurement resolution and enables precise determination of the source of elements, tracking the migration of pollutants down the soil profile. The combination of soil magnetometry and pXRF, supported by the analysis of geochemical indicators, has proven to be a very effective tool in examining soil contamination and environmental site assessment.

Keywords: X-ray spectroscopy, soil magnetometry, soil pollution assessment, geochemical indices, anthropogenic impact

INTRODUCTION

Discriminating between the different origins of metals and metalloids in a soil profile is difficult; however, it is very important in soil pollution studies to distinguish between anthropogenic and natural sources of potentially toxic elements (PTEs), especially in areas where both sources act together. The origin of PTEs can be related to their mobility in the soil environment; the pollutant bonding in anthropogenic particles is usually less stable than in lithogenic minerals (Borůvka et al. 2005). The PTEs are usually transported to the topsoil by industrial and urban dusts, adsorbed on the surface of the technogenic magnetic particles (TMPs) or incorporated into the particle's structure in the form of Fe substitutions. Even in the second case, the inner crystalline structure is non-stoichiometric and it can be more easily destroyed in acidic forest soil than the structure of lithogenic minerals (Magiera et al. 2011, 2021, Bourliva et al. 2017). The secondary particles, originating from pedogenic processes, are very fine, with large surface areas; therefore, they can also adsorb PTEs present in their ionic forms in soil solutions. According to some authors, interaction between soil solutions and the solid phase in polluted systems tends to form more labile associations than in natural (unpolluted) systems. Pollutants are more readily remobilised in such environments (Podlešáková et al. 2001, Borůvka & Vácha 2006). For many years, chemical methods of sequential extraction were used to identify binding forms of PTEs in soil (Mossop & Davidson 2003, Kierczak et al. 2008, Adamo et al. 2018, Magiera et al. 2020). These methods are reliable but extremely labour-intensive and costly; therefore, they are not very effective when used on a larger scale.

Recently, in order to study the spatial distribution of PTEs in soils and identify their origins, the application of geostatistical methods has become very common. Multivariate statistics include principal component analysis (*PCA*) and factor analysis (*FA*) (Zhang et al. 1999, Borůvka et al. 2005, Wang & Qin 2006, Zawadzki et al. 2016). These methods require a large amount of data in order to analyse several factors simultaneously. However, spatial distribution, on its own, is not sufficiently reliable to distinguish between the individual PTE sources. Some additional information about the geological background, soil type, climatic conditions and potential anthropogenic pollution sources (current or historical) must also be gathered. In the absence of in-situ screening techniques in soil investigations, the amount of available data is often too small to enable the application of geostatistics.

For a comprehensive geochemical assessment of the state of the soil environment, including PTE origin, many geochemists have proposed the use of various soil pollution indices (Müller 1969, Håkanson 1980, Gong et al. 2008, Kowalska et al. 2016, 2018, Mazurek et al. 2017). Soil indices are often used in the estimation of environmental risk, as well as the degree of soil degradation (Caeiro et al. 2005, Adamu & Nganje 2010). The most commonly used indices are: geo-accumulation index (I_{geo}), single pollution index (*PI*), enrichment factor (*EF*), contamination factor (*CF*), and pollution load index (*PLI*). Each index has its own strengths and weaknesses; the problem is selecting the most appropriate one in a given research area. In many cases, the use of different indices in the same research area leads to contradictory results (Mazurek et al. 2019). In the case of some pollution indices, it is crucial to determine the geochemical background (Reimann & Garrett 2005, Reimann & de Caritat 2005). Determining the appropriate geochemical background should be based on local soil and site-specific criteria. In order to avoid confusion and uncertainty during soil quality evaluation, a holistic approach should be taken, using local and reference background values to assess the quality of a given soil sample (Kowalska et al. 2018).

The easiest way to indicate the origin of PTEs is to investigate their distribution in vertical soil profiles. In the case of an anthropogenic origin, especially atmospheric deposition, the PTEs mainly accumulate in organic horizons in the topsoil and are closely correlated with TMPs (Szuszkiewicz et al. 2021). In contrast, the content of PTEs of geogenic origin is likely to increase with depth (Magiera et al. 2006, Szuszkiewicz et al. 2016). However, in some soil types, or in cases of old historical pollution, the mobile forms of metals could

have leached downwards, whereas the TMPs stay immobilised in organic horizons. Pedogenic processes may also cause the secondary accumulation of some elements in illuvial soil horizons, often associated with secondary iron minerals (e.g. hematite, goethite, and ferrihydrite), which are detected magnetically in the form of additional magnetic susceptibility peaks (κ). However, this is much smaller than the anthropogenic peak in the uppermost horizon (Magiera et al. 2006). The spatial distribution of PTEs and κ values usually corresponds to the source of enrichment. In the case of lithogenic enrichment, the spatial distribution is related to local geology. Moreover, the spatial distribution pattern of pollution from the local point sources exhibits maxima close to the source, with a decreasing trend with distance from the source (Borůvka et al. 2005). The only effective method with a sufficiently high resolution of soil profile measurements is the combination of soil magnetometry and portable XRF spectroscopy (pXRF). The research objective of this study was to obtain information on the origin of ten PTEs present in the soil at two Natura 2000 protected areas and to check the usefulness of three popular soil indices (I_{geo}, *PI* and *EF*) for assessing soil contamination in the study area.

MATERIALS AND METHODS

Description of the study area

The research was carried out in two forested areas belonging to the Natura 2000 network of European protected areas, located in the Cieszyn region (southern Poland) on the Polish-Czech border (Fig. 1). The first area, 'Las Grabicz' (the Grabicz Forest – LG), is a forest complex located on a hill with a height of 520 m a.s.l., situated 5 km northeast (NE) from the Třinec Iron and Steelworks (on the Czech side of the border), which has operated continuously since 1839 (Magiera et al. 2021). The second area, 'Las Kamieniec' (the Kamieniec Forest – LK), is located on a gentle hill, situated farther to the north, at a distance 9 km NE from the Třinec Iron and Steelworks and 5 km east of the centre of Cieszyn Town.

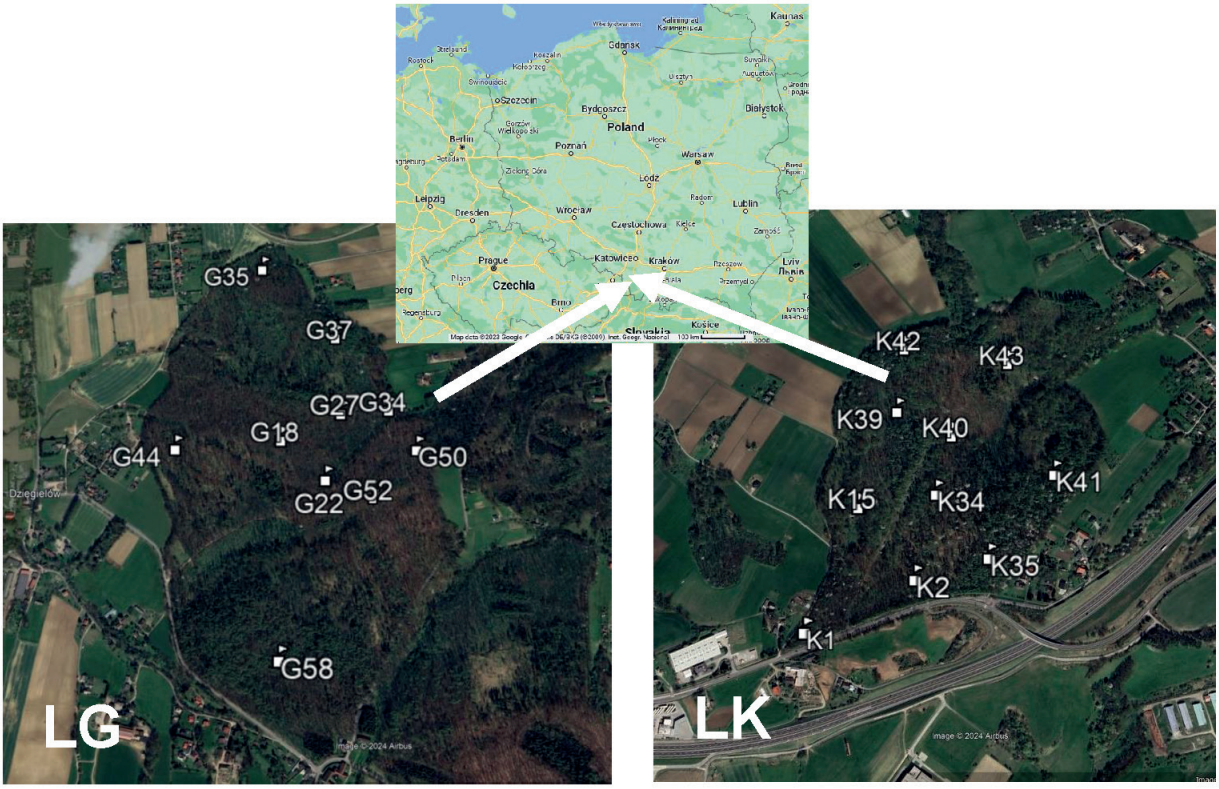

Fig. 1. *Location of research area: LG – the Grabicz Forest, LK – the Kamieniec Forest*

Structurally, both areas belong to the Outer Western Carpathians, in the Mesoregion of the Silesian Foothills (Kondracki 2002). The geology comprises Carpathian flysch formations interspersed with local Teschenite intrusions (a local variety of gabbro) (Różkowski et al. 2020). In both of the studied forest enclaves, there are mainly Eutric and Endoeutric Cambisols, Calcaric Regosols and Rendzic Leptosols. Localised gleysols occur in humid areas and areas of spring outflows. During the research, 30 cm deep topsoil cores were collected but no deep soil pits were established. In all cases, the cores were characterised by a relatively thin layer of undecomposed leaves and slightly decomposed humus. The humic A horizon was usually 13–20 cm thick and mainly consisted of silt or clay with a skeletal fraction of 20–40% (mainly Cieszyn shales). Below this, there was a browning mineral horizon containing clays and loams (usually more than 40% of the skeletal fraction and comprising marly shales and fragments of carbonate rocks).

Soil sampling and laboratory measurements

In 2022, topsoil cores with a diameter of 35 mm were collected from the topsoil (to 30 cm depth), using the HUMAX SH 300 soil sampler equipped with plastic tubes (some cores were shorter due to the shallow bedrock). The sampling network was designed on the basis of previously performed magnetic screening in accordance with ISO 21226:2019 (International Organization for Standardization 2019). In both study areas, 10 points were selected and, in each point, 2 twin cores were collected at a distance of 1 m apart. In total, 40 topsoil core samples were collected and transported to the laboratory of the Institute of Environmental Engineering of the Polish Academy of Sciences in Zabrze (IEE PAS).

Measurement of the vertical distribution of volume magnetic susceptibility (κ) along the core was performed using a Bartington MS2C sensor with a resolution of 1 cm (Fig. 2). The measurement was performed in the laboratory within 7 days after core collection. To prevent drying out, the cores were stored in a fridge. Based on the vertical distribution of κ values, one topsoil core with a more stable magnetic signal was selected for the analysis of nine element contents (As, Cr, Fe, Mn, Pb, Ni, Ti, V and Zn) using an Explorer 7000 portable XRF spectrometer (pXRF) under laboratory conditions following the measurement procedure developed by Magiera & Szuszkiewicz (2025). The detection limit of the methodology and equipment for the analysed elements was as follows (in milligrams per kilogram): As = 2.8, Cr = 18, Fe = 5, Mn = 50, Pb = 3.5, Ni = 8.8, Ti = 50, V = 10, and Zn = 7.5. Selected cores were cut into 2 cm thick slices with a ceramic knife.

Each soil slice after air drying and homogenization was placed in a plastic XRF cup with a thin stretch film instead of a lid. Each sample was measured five times. The instrument was calibrated using standard soil reference materials from the Joint Research Centre, with certified metal concentrations: BCR-142R for light sandy soil. The precision and accuracy parameters for the specified elements determined in three different pXRF procedures and by ICP OES method in relation to the certified metal concentrations in the reference samples (including also BCR-142R) were presented in Magiera and Szuszkiewicz (2025). On the basis of statistical analysis, mean values were calculated after rejecting the outliers.

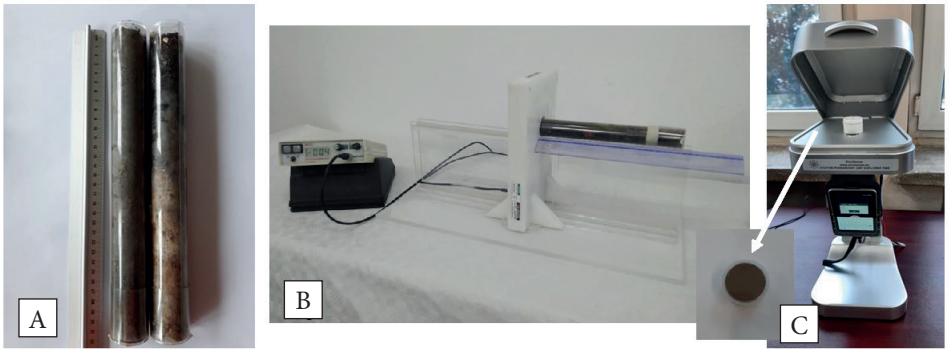

Fig. 2. *Measurement procedure: A) topsoil cores; B) measurement of vertical distribution of κ by MS2C Bartington; C) laboratory measurement of prepared soil sample by pXRF*

Calculation of geochemical indices

Based on the obtained results, three popular geochemical indices of soil contamination with metals and metalloids were calculated: geo-accumulation index (I_{geo}), single pollution index (*PI*) and enrichment index (*EF*).

The I_{geo} index proposed by Müller (1969) defines the soil contamination by a given metal in terms of seven diversified classes. It allows the assessment of soil pollution based on the comparison of PTE content in the topsoil (the O or A horizon) with the geochemical background. I_{geo} values greater than 1.0 indicated an elevated content of heavy metals and soil contamination (Mazurek et al. 2017). The calculation of the index is defined by the following equation:

$$I_{geo} = \log_2\left(\frac{C_n}{1.5C_{GB}}\right) \quad (1)$$

where C_n is the mean value of the element's content, determined in the samples collected from the uppermost 10 cm of the soil core, and C_{GB} is the geochemical background, calculated as the mean value of the element's concentration in the mineral horizon at depths between 24 and 28 cm. Factor 1.5 is the correction factor compensating the natural (lithological) fluctuations in the geochemical data.

The *PI* index is a simple index that can be used to determine which PTE represents the greatest threat to the soil environment. *PI* can be applied for evaluating the degree of individual heavy metal contamination in topsoil and is calculated as the ratio of C_n and C_{GB}:

$$PI = \frac{C_n}{C_{GB}} \quad (2)$$

The *EF* factor is used to assess the possible impact of anthropogenic activities on the heavy metal concentrations in the soil. In order to identify the expected effect of anthropogenesis, it was calculated based on the TOP/BOT method described by Reimann and de Caritat (2005), using the following equation:

$$EF = \frac{C_n / L_v}{C_{GB} / L_{vGB}} \quad (3)$$

where C_n is the mean content of the analysed element in the uppermost 10 cm of soil core, C_{GB} is the geological background, calculated as the mean value of the element at the depths between 24 and 28 cm, and L_v is the mean content of the element used as a reference in the uppermost 10 cm; L_{vGB} is the content of the reference element at depths ranging from 24 to 28 cm. In our study, Fe was used as the reference element because of its low variability in the studied soil profiles (Figs. 3, 4).

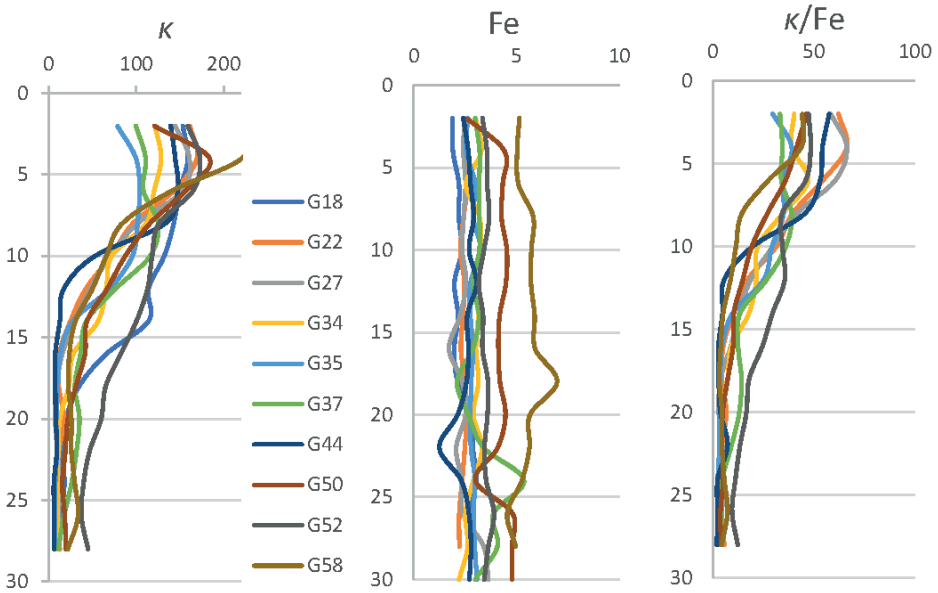

Fig. 3. *Values of volume magnetic susceptibility κ [·10^{-5} SI units], Fe content [%] and κ/Fe ratio in topsoil cores in the Grabicz Forest (LG)*

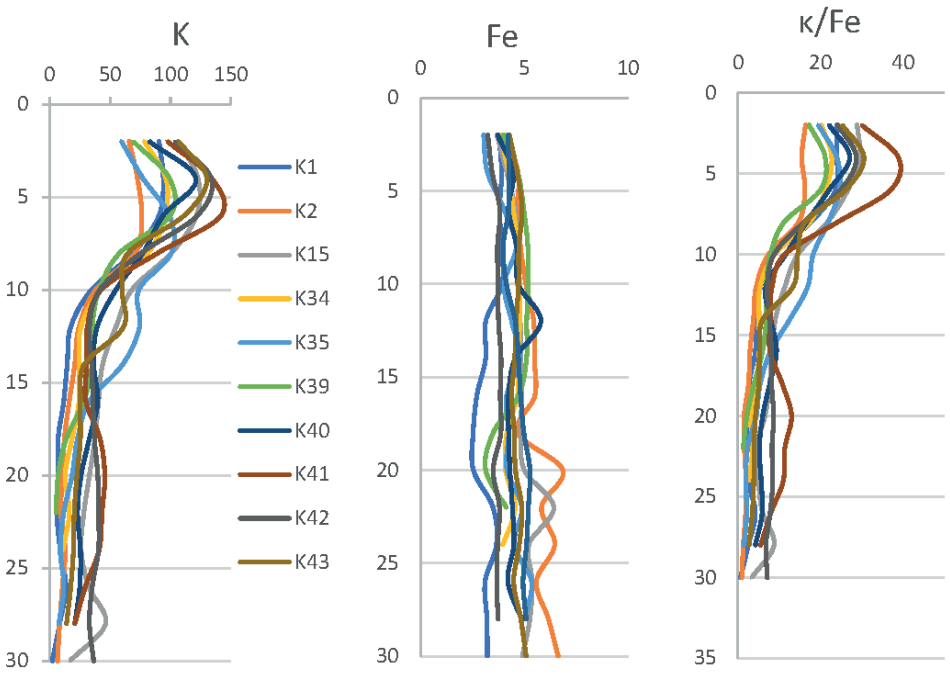

Fig. 4. *Values of volume magnetic susceptibility κ [·10^{-5} SI units], Fe content [%] and κ/Fe ratio in topsoil cores in the Kamieniec Forest (LK)*

If the *EF* ranges from 0.5 to 1.5, it means that the content of that particular element in the soil is most probably caused by natural processes. However, if the value of *EF* exceeds 1.5, there is a high probability that the content of PTE in the soil is enriched due to anthropogenic activities (Gong et al. 2008, Hu et al. 2013, Mazurek et al. 2017, Kowalska et al. 2018).

RESULTS AND DISCUSSION

Visual assessment of all the collected soil cores showed similar morphological features in the studied forest soils. They can mostly be described as Cambisols or Skeleti-Calcaric Cambisols, developed on Cretaceous Cieszyn marly shales and marls. All of them were characterised by a relatively thin (2–6 cm) layer of undecomposed leaves and mull humus in the surface layer. Below that, there was an Ah horizon, to an approximate depth of 12–18 cm, composed mainly of silt or clay with a skeletal fraction below 40%. This was followed by a B horizon containing silt and clay, usually more than 40% of the skeletal fraction being composed of marly shales and carbonate rock fragments. The vertical distribution of κ values showed a significant magnetic enhancement in the upper part of the core, in the organic soil horizon (Figs. 3, 4). Full data on the vertical distribution of magnetic susceptibility values in soil cores are provided in the Tables S1 and S2 attached as a supplementary file in the online version. The maximum magnetic susceptibility was usually located between 2 and 6 cm. Only in core G37, the maximum κ was shifted down to 9 cm depth. In LG cores, the maximum κ was in the range of (80–220) · 10^{-5} SI units; whereas, in LK cores, the observed maximum κ values were slightly lower (less than 130 · 10^{-5} SI units). In the lower parts of the cores in the B horizon (26–30 cm), these values usually dropped to less than 10 · 10^{-5} SI units; however, in some cores (G50, G52, G58, K40, K41, K42, K43) it still remained above 15 · 10^{-5} SI units. Relatively high κ values in the uppermost part of the soil core were of anthropogenic origin, related to the accumulation of TMPs from dust deposition in the organic horizon (Magiera et al. 2006, Błońska et al. 2016, Szuszkiewicz et al. 2021). In all the examined cores, there was a typical wide magnetic peak, characterising Cambisols developed under a deciduous tree stand with a strong anthropogenic effect and the dominance of ferrimagnetic forms of iron in the upper part of the soil profile (Magiera et al. 2006, 2019).

Table 1
Correlation coefficients between magnetic susceptibility values and analyzed metals and metalloids in soil from the Grabicz Forest

Core no.	Ti	V	Cr	Mn	Fe	Ni	Zn	As	Pb
κ in G18	**−0.956**	**−0.960**	**−0.900**	0.598	**−0.776**	−0.953	**0.963**	**0.929**	**0.938**
κ in G22	**−0.966**	**−0.969**	**−0.936**	0.084	0.563	−0.948	**0.971**	**0.952**	**0.974**
κ in G27	**−0.906**	**−0.899**	**−0.869**	**0.692**	0.067	−0.828	**0.971**	**0.966**	**0.978**
κ in G34	**−0.896**	**−0.874**	**−0.864**	0.475	0.215	−0.887	**0.990**	**0.981**	**0.989**
κ in G35	**−0.901**	**−0.873**	**−0.832**	−0.158	0.015	−0.736	**0.926**	**0.958**	**0.963**
κ in G37	−0.593	**−0.603**	−0.578	**0.724**	−0.278	−0.365	**0.960**	**0.926**	**0.967**
κ in G44	**−0.940**	**−0.959**	**−0.880**	0.333	0.261	−0.698	**0.989**	**0.985**	**0.991**
κ in G50	0.013	−0.206	−0.302	0.097	−0.083	0.773	**0.984**	**0.910**	**0.940**
κ in G52	−0.492	**−0.631**	**−0.662**	0.247	−0.318	−0.643	**0.905**	**0.908**	**0.929**
κ in G58	0.225	−0.185	−0.399	0.398	−0.368	−0.600	**0.936**	**0.911**	**0.932**

The Fe content in the studied cores was between 2 and 6% in both the LG and LK areas; the vertical distribution of the measured Fe values was stable along the cores, especially in the upper horizons (O and Ah). In these horizons, the coefficient of variability (*CV*) did not exceed 9%. In the B horizon there were thin layers in some profiles, where the total Fe content increased up to 7% or decreased below 1.5%. Despite these fluctuations, the average *CV* for Fe content in the LG profiles was 12.4% and, for LK, it was 10.5% (the lowest among the investigated elements) (Figs. 3, 4). In the cores from both areas, a relationship between κ values and most of the analyzed elements is observed, as reflected in the correlation coefficients (Tables 1, 2).

Table 2
Correlation coefficients between magnetic susceptibility values and analyzed metals and metalloids in soil from the Kamieniec Forest

Core no.	Ti	V	Cr	Mn	Fe	Ni	Zn	As	Pb
κ in K1	−0.177	−0.454	−0.579	0.441	**0.704**	−0.467	**0.865**	**0.881**	**0.922**
κ in K2	−0.370	−0.588	**−0.762**	0.133	**−0.758**	**−0.628**	**0.972**	**0.894**	**0.969**
κ in K15	**−0.659**	**−0.670**	**−0.768**	**0.740**	**−0.701**	**−0.746**	**0.897**	**0.901**	**0.944**
κ in K34	−0.223	−0.453	−0.541	0.304	−0.053	0.238	**0.979**	**0.960**	**0.986**
κ in K35	−0.214	−0.402	−0.471	0.577	−0.458	**0.756**	**0.940**	**0.938**	**0.956**
κ in K39	0.428	0.153	−0.071	0.596	0.462	−0.324	**0.926**	**0.897**	**0.855**
κ in K40	−0.448	−0.503	**−0.619**	0.446	−0.205	0.485	**0.947**	**0.947**	**0.958**
κ in K41	**−0.628**	**−0.689**	**−0.615**	0.276	−0.424	−0.479	**0.957**	**0.943**	**0.962**
κ in K42	−0.588	**−0.727**	**−0.629**	0.747	0.073	0.326	**0.960**	**0.928**	**0.957**
κ in K43	−0.378	**−0.647**	**−0.803**	−0.053	**−0.810**	**−0.798**	**0.944**	**0.954**	**0.988**

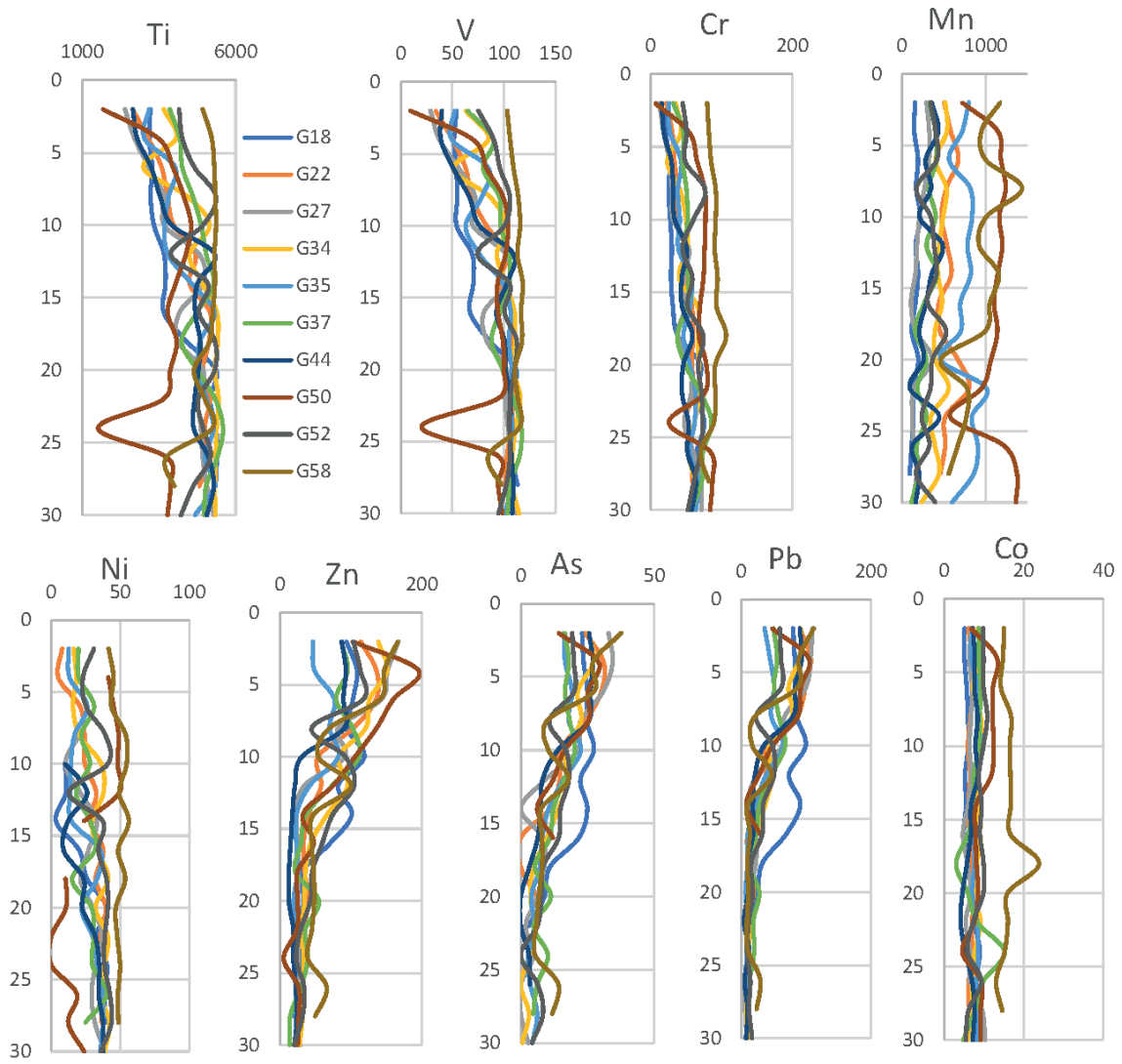

Fig. 5. *Metals and metalloids contents [mg · kg^{-1}] in topsoil cores (0–30 cm depth) in the area of the Grabicz Forest (LG)*

Low and, sometimes even negative, correlations between κ and the total Fe content, observed in many soil profiles (Tables 1, 2), clearly suggest that iron occurs in different forms of magnetic iron-bearing minerals in the tested soils. The other calculated parameter, κ/Fe, is a measure of the share of ferrimagnetic forms of iron oxides in the total iron content of the soil profile (Szuszkiewicz et al. 2016). Despite the fact that the distribution of Fe content in the measured soil cores was relatively stable and, in most cases, slightly higher Fe contents were recorded in the lower part of the profile (B horizon), in the case of the κ/Fe ratio, significantly higher values were observed in the upper part of the profile (O and Ah horizons). The maximum values of this parameter corresponded to the magnetic peak observed in the organic horizon (Figs. 3, 4). This means that the magnetic signal in the upper part of the soil profile was controlled by the ferrimagnetic fraction related to the accumulation of TMPs in the organic horizon. In the lower part of the profile (mainly the B horizon), iron was associated with paramagnetic or antiferrimagnetic minerals and the Fe fluctuations observed in the B horizon were related to the pedogenic precipitation of iron hydroxides or, more likely, the presence of layers with different clay mineral contents.

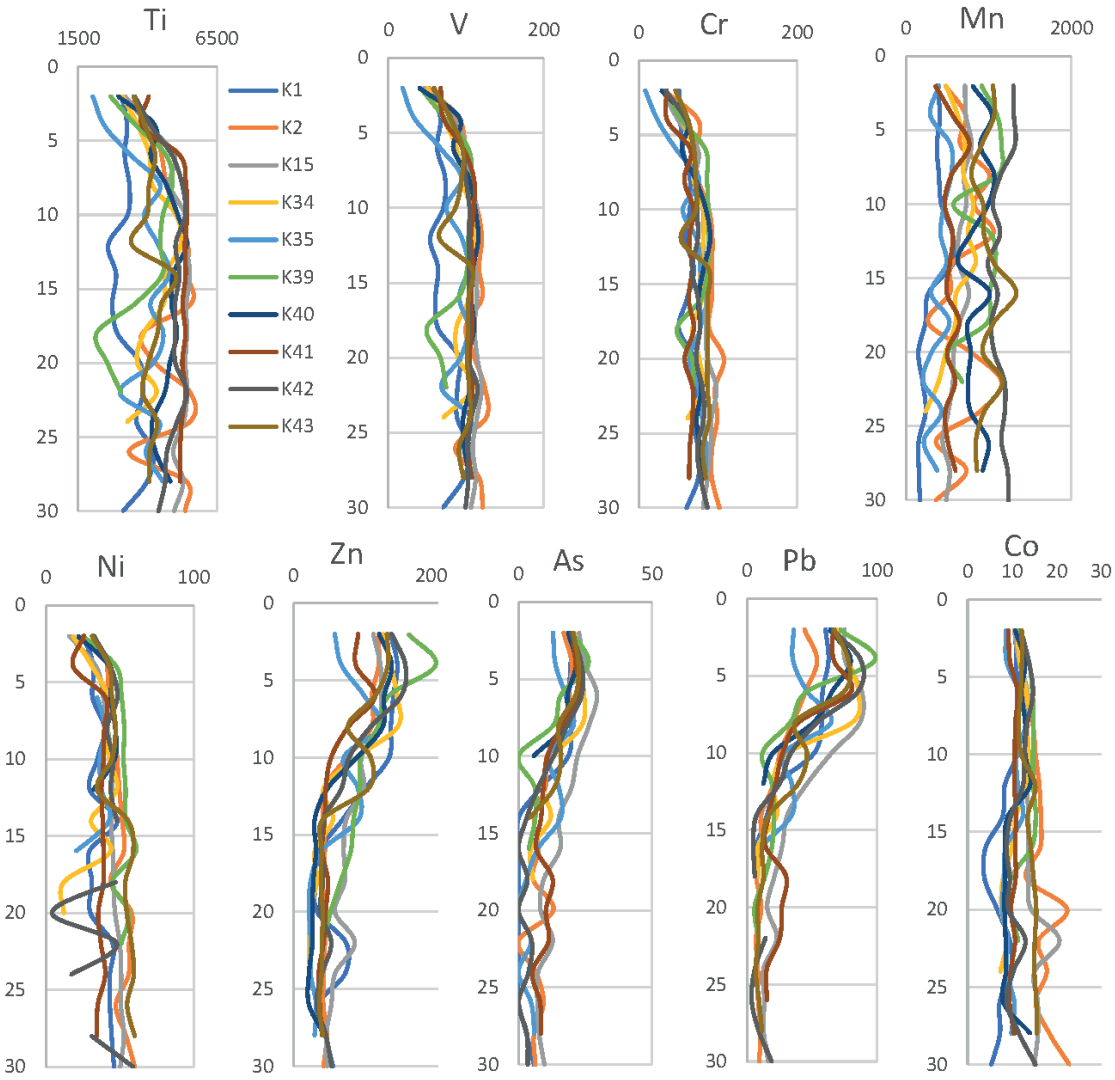

Fig. 6. *Metals and metalloids contents [mg · kg^{-1}] in topsoil cores (0–30 cm depth) in the area of Kamieniec Forest (LK)*

The highly stable iron content along the measured profiles was the reason that this element was selected as a reference element for the calculation of the *EF* index. Analyses of the vertical distribution of Zn, Pb and As have shown great similarities to the vertical distribution of κ values, which clearly indicates the anthropogenic nature of these elements. In the LG area, the correlation coefficients between the κ value and the Pb, Zn and As contents were, respectively: 0.93–0.99 for Pb and 0.91–0.99 for Zn and As (Table 1).

Slightly lower correlation coefficients were recorded for the LK area (0.86–0.99 for Pb, 0.87–0.98 for Zn and 0.88–0.95 for As) (Table 2). The highest content of these elements was found in the humus layer or upper part of the Ah horizon, at a depth of 2–10 cm, and the maximum content of Zn in particular layers, was approximately 200 mg/kg. Maximum Pb content was approximately 100 mg/kg, whereas the maximum As content in the LG area did not exceed 40 mg/kg, and 30 mg/kg in the LK area (Figs. 5, 6). In all cases, these values were much lower than the limits (Zn = 1000 mg/kg, Pb = 500 mg/kg, As = 50 mg/kg) specified in the Regulation of the Minister of the Environment for assessing land pollution on group II lands, including protected areas (national parks and nature reserves) (Rozporządzenie 2016)

The As and Pb content in the lower, mineral, part of the profile was very low, sometimes below the detection limit of the pXRF meter. In some profiles, the maximum concentration of Zn, Pb and As were observed slightly below the κ maximum or were observed as an additional peak in the upper part of the Ah horizon. This suggests a partial downward migration of these elements, which was also reported by other authors (Gregorauskienė & Kadunas 2005, Fernandez et al. 2007, García-Sánchez et al. 2010). These authors also pointed at the strong affinity of these metals with soil organic matter. Wawer (2020) pointed out that the content of Zn and Pb originating from fly ash emitted by the power plant and deposited in its vicinity was at its highest in the organic horizon.

In the case of Ni, the situation was the opposite and, in the humus layer, the content of this element was below the detection limit of the pXRF, while the maximum values in the lower part of the profile were 37–50 mg/kg in the LG area and 40–60 mg/kg in the LK area. At the points located on the highest parts of the LG hill (points G52 and G58), as well as those located on the southwestern slope (point G44), also in the upper part of the profile, Ni concentrations increased, reaching 56 mg/kg. This also suggests a partially anthropogenic nature, relating to historical emissions from the Třinec Steelworks. In the LK area, the distribution of Ni content in the soil cores was less diverse (Fig. 6). The investigated soils showed surprisingly high contents of Cr (more than 100 mg/kg in some profiles), V (up to 135 mg/kg) and Ti (more than 5000 mg/kg), while the average content of these elements in the Polish soils was 6 mg/kg, 8 mg/kg and 34 mg/kg, respectively (Lis & Pasieczna 1995). All these elements had a similar distribution in the soil profile, showing a definite geogenic character, with maximum concentrations in the mineral horizon, a tendency to increase down the soil profile and high negative correlations with the κ value (Tables 1, 2).

The source of chromium is most likely the Cieszyn Shales which occur in the regional bedrock, with Cr content of 120–280 mg/kg; its source mainly being the clay minerals (Gucwa & Pelczar 1972). The content of the clay fraction in the mineral part of the tested soils exceeded 40%. There are also teschenites in this area, which is the local igneous rock, with Cr content up to 1050 mg/kg. The release of this metal, as a result of hypergenic processes and migration in the environment, may also affect its content in the investigated soils. Cieszyn Shales may also be a source of titanium, with contents of 2000–8000 mg/kg. The origin of vanadium is not fully explained. The vertical distribution in the soil profile (almost identical to that of Cr and Ti) suggests the same geogenic source. Nevertheless, the data in the literature indicates that V in both the Cieszyn Shales and the carbonate rocks in this region only occurs in trace amounts. The occurrence of vanadium could be explained by the presence of siderite inclusions in the Cieszyn Shales, which may contain higher V concentrations, but this has not yet been confirmed by geochemical studies. Additional data on the vertical distribution of metals and metalloids in soil cores are provided in the Tables S3–S22 (attached as a supplementary file in the online version).

The Mn content in the tested soil profiles varied greatly. The maximum contents of this element ranged from approximately 200 mg/kg to above 1400 mg/kg and, even within one profile, the differences were quite significant. The maximum contents were observed in different layers, both in the mineral and humus horizons (Figs. 5, 6). In most profiles, there is no correlation of Mn content with magnetic parameters but there are also profiles where the correlation coefficients between these values are greater than 0.50 (profiles G18, G27, G37, K15, K35, K39, K42). As some indices have shown minimal or medium contamination, this may suggest a partially anthropogenic origin of this element in the studied areas. Iron metallurgy was often reported as the source of manganese (Reimann & de Caritat 2005, Sajn 2005, Jabłońska et al. 2021). As for natural sources, increased Mn contents are recorded in the diagenetic binder of carbonate rocks found in the subsurface.

Although the maximum PTE contents in the organic horizon of the investigated soil cores were significantly below the threshold values of both Polish national thresholds for soils in forests and protected areas (Rozporządzenie 2016), as well as those requiring the action level given in international standards (Reimann & de Caritat 2005), the I_{geo} indices exhibited moderately to heavily contaminated soil for As and Pb contents in most of the soil profiles. According to this index, the soil was moderately to heavily polluted with Pb in 70%

of LG and 50% of LK and As in 50% of LG and 20% of LK. Moreover, at points G18 and G22, the value of the I_{geo} for As indicates highly contaminated soil (Tables 3, 4). The geo-accumulation index allows for the assessment of individual PTE pollution, based on the comparison of the element's content in the O or A horizon with the geochemical background of the soils (Müller 1969, Gong et al. 2008, Kowalska et al. 2016). The applied background values are crucial for these calculations (Reimann & Garrett 2005). Usually, geochemists use the regional or local background values taken from the archive data or measure the general bedrock value for the whole area. This procedure is obvious if only the uppermost topsoil layer is sampled for the site assessment. Such a calculated I_{geo} does not take into account the natural geochemical variability at a regional or local scale. Even the application of the correction factor of 1.5 in the equation did not fully compensate the natural (lithological) fluctuations in the geochemical data. The proper selection of the geochemical background is even more important in the calculation of the *PI*. It is very simple and only expressed by the ratio of the measured element content to the geochemical background, without any correction factor compensating the background fluctuations.

Table 3
Geo-accumulation index (I_{geo}) of top soil samples collected in the Grabicz Forest

Core no.	Ti	V	Cr	Mn	Fe	Zn	As	Pb	Ni
G18	–1.31	–1.62	–1.98	0.03	–0.99	1.54	3.36	2.66	–3.10
G22	–1.12	–1.38	–1.34	–0.44	–0.45	1.15	3.71	2.56	–1.76
G27	–1.25	–1.59	–1.89	0.35	–0.74	1.76	1.56	2.89	0.26
G34	–0.98	–1.08	–1.19	–0.25	–0.40	1.32	2.41	2.19	0.77
G35	–1.13	–1.29	–1.39	–0.80	–0.63	0.95	1.47	1.87	–0.70
G37	–0.88	–0.93	–1.35	0.15	–0.79	1.19	1.52	1.69	–0.97
G44	–1.22	–1.56	–1.70	–0.26	–0.53	1.25	2.07	2.49	–3.08
G50	–0.67	–0.97	–1.19	–0.86	–0.83	1.84	0.54	2.71	n/a
G52	–0.66	–0.75	–0.86	–0.13	–0.65	1.08	1.06	1.17	–0.97
G58	–0.31	–0.44	–0.49	0.15	–0.46	0.58	1.32	2.10	–0.62

Legend: $I_{geo} \leq 0$ – unpolluted (green); $I_{geo} = 0–1$ – unpolluted to moderately polluted (yellow); $I_{geo} = 1–2$ – moderately polluted (orange); $I_{geo} = 2–3$ – moderately to heavily polluted (red); $I_{geo} = 3–4$ – highly contaminated (purple); n/a – no data.

Table 4
Geo-accumulation index (I_{geo}) of top soil samples collected in the Kamieniec Forest

Core no.	Ti	V	Cr	Mn	Fe	Zn	As	Pb	Ni
K1	–0.87	–1.16	–0.92	0.52	–0.37	1.05	1.56	2.76	–0.46
K2	–0.92	–1.00	–1.05	–0.43	–0.97	0.71	0.89	1.57	–0.60
K15	–0.76	–0.88	–1.07	0.01	–0.84	0.65	1.04	1.87	–0.55
K34	–0.48	–0.72	–0.83	0.25	–0.52	1.95	0.93	2.37	n/a
K35	–0.99	–1.44	–1.56	–0.19	–0.97	0.97	1.26	2.64	n/a
K39	0.07	–0.16	–0.41	–0.16	–0.17	0.83	1.33	1.87	–0.73
K40	–0.65	–0.80	–0.94	–0.49	–0.64	1.48	1.85	1.93	n/a
K41	–0.71	–0.79	–0.90	–0.55	–0.63	0.60	0.77	1.00	–0.75
K42	–0.57	–0.80	–0.95	–0.57	–0.63	0.95	2.17	2.04	n/a
K43	–0.66	–0.82	–0.98	–0.48	–0.86	0.96	2.62	2.13	–0.44

Legend: $I_{geo} \leq 0$ – unpolluted (green); $I_{geo} = 0–1$ – unpolluted to moderately polluted (yellow); $I_{geo} = 1–2$ – moderately polluted (orange); $I_{geo} = 2–3$ – moderately to heavily polluted (red); $I_{geo} = 3–4$ – highly contaminated (purple); n/a – no data.

In our case, by applying the pXRF technique in combination with soil magnetometry, we could measure the PTE content and their vertical distribution in the topsoil to 30 cm depth. Therefore, we avoided the problem of natural geochemical variability in the local geochemical background by using the TOP/BOT-ratio method by Reimann and Garrett (2005). In this case, the background value is more realistic than the one average background calculated for the whole study area. By analysing the variability of PTE contents in the topsoil profile continuously (with a relatively high resolution down to 30 cm depth), we avoided misinterpreting the natural biogeochemical soil formation processes in soil horizons, which was the main critical argument against using this method (Reimann & Garrett 2005).

The data presented in Tables 3–8 suggest that the values of *PI* index are overestimated, in relation to the other calculated geochemical indices (I_{geo} and *EF*), which seem more reliable. According to *PI*, 80% of our soil samples were very heavily polluted with Pb and most of them were also highly or heavily polluted by As and Zn, in contradiction with other parameters. The *PI* also suggests that soils throughout the LK area and most of the LG area were at least slightly polluted with Mn and Co.

Table 5
Pollution index (PI) of top soil samples collected in the Grabicz Forest

Core no.	Ti	V	Cr	Mn	Fe	Zn	As	Pb	Ni
G18	0.61	0.49	0.38	1.53	0.76	4.36	15.44	9.47	0.18
G22	0.69	0.57	0.59	1.11	1.10	3.34	19.68	8.83	0.44
G27	0.63	0.50	0.41	1.91	0.90	5.07	4.41	11.12	1.80
G34	0.76	0.71	0.66	1.26	1.14	3.75	7.96	6.87	2.56
G35	0.68	0.61	0.57	0.86	0.97	2.90	4.16	5.49	0.92
G37	0.82	0.79	0.59	1.67	0.87	3.41	4.30	4.84	0.77
G44	0.65	0.51	0.46	1.26	1.04	3.57	6.29	8.43	0.18
G50	0.94	0.76	0.66	0.83	0.84	5.36	2.18	9.81	n/a
G52	0.95	0.89	0.83	1.37	0.95	3.17	3.12	3.38	0.77
G58	1.21	1.11	1.07	1.67	1.09	2.24	3.75	6.42	0.98

Legend: *PI* < 1 – unpolluted (green); *PI* = 1–2 – slightly polluted (yellow); *PI* = 2–3 – moderately polluted (orange); *PI* = 3–5 – highly polluted (red); *PI* > 5 – very heavily polluted (purple); n/a – no data.

Table 6
Pollution index (PI) of top soil samples collected in the Kamieniec Forest

Core no.	Ti	V	Cr	Mn	Fe	Zn	As	Pb	Ni
K1	0.82	0.67	0.79	2.16	1.16	3.11	4.43	10.19	1.09
K2	0.80	0.75	0.72	1.11	0.77	2.46	2.78	4.46	0.99
K15	0.89	0.82	0.71	1.51	0.84	2.36	3.08	5.49	1.03
K34	1.07	0.91	0.84	1.79	1.05	5.78	2.85	7.74	n/a
K35	0.75	0.55	0.51	1.31	0.76	2.95	3.59	9.37	n/a
K39	1.58	1.35	1.13	1.34	1.34	2.66	3.76	5.49	0.91
K40	0.95	0.86	0.78	1.07	0.96	4.18	5.41	5.70	n/a
K41	0.92	0.87	0.81	1.03	0.97	2.27	2.56	3.01	0.89
K42	1.01	0.86	0.77	1.01	0.97	2.90	6.77	6.17	n/a
K43	0.95	0.85	0.76	1.08	0.83	2.92	9.23	6.59	1.11

Legend: *PI* < 1 – unpolluted (green); *PI* = 1–2 – slightly polluted (yellow); *PI* = 2–3 – moderately polluted (orange); *PI* = 3–5 – highly polluted (red); *PI* > 5 – very heavily polluted (purple); n/a – no data.

Table 7
Enrichment factor (EF) of top soil samples collected in the Grabicz Forest

Core no.	Ti	V	Cr	Mn	Zn	As	Pb	Ni
G18	0.80	0.65	0.50	2.03	5.78	20.44	12.53	0.23
G22	0.63	0.52	0.54	1.01	3.03	17.90	8.03	0.40
G27	0.70	0.55	0.45	2.12	5.64	4.91	12.36	2.01
G34	0.66	0.62	0.58	1.10	3.29	6.98	6.02	2.25
G35	0.70	0.63	0.59	0.89	2.99	4.29	5.66	0.95
G37	0.94	0.91	0.68	1.92	3.94	4.97	5.59	0.88
G44	0.62	0.49	0.44	1.21	3.45	6.07	8.13	0.17
G50	1.12	0.91	0.78	0.98	6.38	2.59	11.66	n/a
G52	1.00	0.94	0.87	1.43	3.32	3.28	3.54	0.80
G58	1.11	1.01	0.98	1.53	2.05	3.45	5.89	0.90

Legend: $EF \leq 2.0$ – geogenic origin (green); $EF = 2–5$ – medium anthropogenic enrichment (yellow); $EF = 5–20$ – significant anthropogenic enrichment (orange); $EF > 20$ – very high anthropogenic enrichment (red); n/a – no data.

Table 8
Enrichment factor (EF) of top soil samples collected in the Kamieniec Forest

Core no.	Ti	V	Cr	Mn	Zn	As	Pb	Ni
K1	0.71	0.58	0.68	1.85	2.68	3.81	8.76	0.94
K2	1.04	0.98	0.94	1.45	3.20	3.63	5.82	1.29
K15	1.06	0.98	0.85	1.80	2.82	3.68	6.55	1.22
K34	1.03	0.87	0.81	1.71	5.52	2.73	7.40	n/a
K35	0.99	0.72	0.66	1.72	3.86	4.69	12.26	n/a
K39	1.18	1.00	0.84	1.01	1.99	2.81	4.11	0.68
K40	0.99	0.89	0.81	1.11	4.34	5.62	5.92	n/a
K41	0.95	0.90	0.83	1.06	2.35	2.64	3.10	0.92
K42	1.04	0.89	0.80	1.04	2.99	6.98	6.36	n/a
K43	1.15	1.03	0.92	1.30	3.53	11.18	7.98	1.34

Legend: $EF \leq 2.0$ – geogenic origin (green); $EF = 2–5$ – medium anthropogenic enrichment (yellow); $EF = 5–20$ – significant anthropogenic enrichment (orange); $EF > 20$ – very high anthropogenic enrichment (red); n/a – no data.

According to the *PI* calculated for cores G58 and K39, the soil was slightly polluted with all the elements considered. The third analysed index, *EF*, better explains the problem, as it is not defined as a measure of pollution but an indicator of the possible impact of anthropogenic activities on the PTEs concentrations in the soil. It was proposed in order to identify the expected effect of anthropogenesis on PTE accumulation. Calculation of the *EF* requires the proper selection of both a geological background and a reference element. The reference element has to be characterised by a low variability in its concentration within the soil profile (Elias & Gbadegesin 2011, Kowalska et al. 2016). In the case of using pXRF, its content must be relatively high, above the detection limit for this method. In our study, we considered three elements (Fe, Mn and Ti) as the reference elements. Because of the high stability in the soil cores investigated, Fe was finally used as a reference element in the calculation of the *EF*.

According to *EF*, three PTEs (Pb, As and Zn) showed values more than 2.0, indicating anthropogenic enrichment in all of the studied soil cores. There was only one exception to this: in core K39, the *EF* was 1.99. In the case of Pb, significant anthropogenic enrichment was observed in 9 soil cores collected in the LG area and 8 cores

collected in the LK area. In the case of As, the highest *EF* value was calculated for core G18, with a value more than 20, which indicates a very high anthropogenic enrichment. In the case of the remaining cores, the anthropogenic enrichment in As and Zn was medium or significant (Tables 7, 8). In cores G18 and G27, the *EF* for Mn was slightly above 2.0, which suggests that the applied background values have a possibly anthropogenic nature in some parts of the studied areas.

CONCLUSIONS

The use of a pXRF spectrometer allows the assessment of the distribution of PTEs in the soil profile with high measurement resolution and enables precise determination of the source of these elements, tracking the migration of pollutants down the soil profile. Such information cannot be obtained effectively using ICP or other expensive and time-consuming chemical methods that require the digestion of a soil sample.

The vertical distribution of magnetic susceptibility (κ) showed significant magnetic enhancement in the upper part of the cores which was caused by the accumulation of TMPs in the organic soil horizon. The typical anthropogenic peak of κ values strongly correlates with the Pb, As and Zn contents, confirming the anthropogenic origin of these PTEs in the soil from both studied areas. Although the distribution of Fe along the soil profile is relatively stable, various forms of iron mineralogy were detected by analysing the κ/Fe ratio. This parameter was significantly higher in the upper part of the profile (O and Ah horizons) and meant that the magnetic signal in the upper part of the soil profile was controlled by the technogenic ferrimagnetic fraction of iron oxides deposited from the air during a long period of human activity (industrial and urban emissions) in this area. Antiferromagnetic and paramagnetic iron minerals predominate in the mineral horizons and their distribution is controlled by natural lithogenic and pedogenic processes. The possibility of the downward migration of anthropogenic elements, such as Zn, Pb and As, was observed in some profiles, where their maximum concentration was observed in the Ah horizon, below the anthropogenic magnetic peak. In the case of Mn, the dual nature of its origin was observed (partly anthropogenic and partly natural). The distribution pattern of the remaining studied elements (Ti, V, Cr, Co and Ni) in the soil profile and the analysis of geochemical indices (I_{geo}, *PI* and *EF*) suggested their lithogenic and/or pedogenic origins, related to the increased concentration of these elements in the geological bedrock (Cieszyn Shales) and they are controlled by hypergenic processes which cause the PTEs to be released from the bedrock.

The measured contents of all investigated PTEs were far below the threshold values which would require any action or soil remediation; however, the geochemical indices indicated moderately or even highly polluted soil. The *PI* index, based on simple concentration ratios of individual elements, was overestimated and, in the context of other results, unreliable. The other two tested geochemical indices (I_{geo} and *EF*) should be considered in terms of the anthropogenic or natural origin of the PTEs in the studied soil profiles, rather than as pollution indicators. This interpretation should be supported by a detailed analysis of the variability of PTEs in the topsoil profile and the location of their maximum concentration in the profile, in relation to soil morphology and individual soil horizons. The combination of soil magnetometry and pXRF spectroscopy, supported by the analysis of geochemical indices such as *EF* or I_{geo}, is a very effective tool in soil pollution studies and environmental site assessments.

Author contributions: Tadeusz Magiera: conceptualization, project administration, methodology, writing original draft, final data interpretation. Małgorzata Wawer-Liszka: field measurement, statistical analysis, data visualization.

Declaration of competing interest: The authors declare that they have no known competing financial interests or personal relationships that could have influenced the work reported in this paper.

Acknowledgements: The study was supported by a subsidy from the Polish Ministry of Education and Science for the Institute of Environmental Engineering, Polish Academy of Sciences in the frame of statutory works no. 1a – 134/21. The authors would like to thank the professional Proof-Reading-Services.com for language corrections.

REFERENCES

Adamo P., Agrelli D. & Zampella M., 2018. Chemical speciation to assess bioavailability, bioaccessibility and geochemical forms of potentially toxic metals (PTMs) in polluted soils. [in:] De Vivo B., Belkin H.E. & Lima A. (eds.), *Environmental Geochemistry: Site Characterization, Data Analysis and Case Histories*, Elsevier, 153–194. https://doi.org/10.1016/B978-0-444-63763-5.00010-0.

Adamu C.L. & Nganje T.N., 2010. Heavy metal contamination of surface soil in relationship to land use patterns: A case study of Benue State, Nigeria. *Materials Sciences and Applications*, 1(3), 127–134. https://doi.org/10.4236/msa.2010.13021.

Błońska E., Lasota J., Szuszkiewicz M., Łukasik A. & Klamerus-Iwan A., 2016. Assessment of forest soil contamination in Krakow surroundings in relation to the type of stand. *Environmental Earth Sciences*, 75(16), 1205. https://doi.org/10.1007/s12665-016-6005-7.

Borůvka L. & Vácha R., 2006. Litavka river alluvium as a model area heavily polluted with potentially risk elements. [in:] Morel J.L., Echevarria G. & Goncharova N. (eds.), *Phytoremediation of Metal-Contaminated Soils*, Springer, Dordrecht, 267–298. https://doi.org/10.1007/1-4020-4688-X_9.

Borůvka L., Vacek O. & Jehlička J., 2005. Principal component analysis as a tool to indicate the origin of potentially toxic elements in soils. *Geoderma*, 128(3–4), 289–300. https://doi.org/10.1016/j.geoderma.2005.04.010.

Bourliva A., Papadopoulou L., Aidona E., Giouri K., Simeonidis K. & Vourlias G., 2017. Characterization and geochemistry of technogenic magnetic particles (TMPs) in contaminated industrial soils: Assessing health risk via ingestion. *Geoderma*, 295, 86–97. https://doi.org/10.1016/j.geoderma.2017.02.001.

Caeiro S., Costa M.H., Ramos T.B., Fernandes F., Silveira N. & Coimbra A., 2005. Assessing heavy metal contamination in Sado Estuary sediment: An index analysis approach. *Ecological Indicators*, 5(2), 151–169. https://doi.org/10.1016/j.ecolind.2005.02.001.

Elias P. & Gbadegesin A., 2011. Spatial relationships of urban land use, soils and heavy metal concentrations in Lagos Mainland Area. *Journal of Applied Sciences and Environmental Management*, 15(2), 391–399. https://doi.org/10.4314/jasem.v15i2.68533.

Fernandez C., Labanowski J., Cambier P., Jongmans A.G. & van Oort F., 2007. Fate of airborne metal pollution in soils as related to agricultural management. 1. Zn and Pb distributions in soil profiles. *European Journal of Soil Science*, 58(3), 547–559. https://doi.org/10.1111/j.1365-2389.2006.00827.x.

García-Sánchez A., Alonso-Rojo P. & Santos-Francés F., 2010. Distribution and mobility of arsenic in soils of a mining area (Western Spain). *Science of the Total Environment*, 408(19), 4194–4201. https://doi.org/10.1016/j.scitotenv.2010.05.032.

Gregorauskienė V. & Kadunas V., 2006. Vertical distribution patterns of trace and major elements within soil profile in Lithuania. *Geological Quarterly*, 50(2), 229–237.

Gong Q., Deng J., Xiang Y., Wang Q. & Yang L., 2008. Calculating pollution indices by heavy metals in ecological geochemistry assessment and a case study in parks of Beijing. *Journal of China University of Geosciences*, 19(3), 230–241. https://doi.org/10.1016/S1002-0705(08)60042-4.

Gucwa I. & Pelczar A., 1972. Geochemia warstw cieszyńskich Śląska Cieszyńskiego. *Geological Quarterly*, 16(2), 405–419.

Håkanson L., 1980. An ecological risk index for aquatic pollution control: A sedimentological approach. *Water Research*, 14(8), 975–1001. https://doi.org/10.1016/0043-1354(80)90143-8.

Hu Y., Liu X., Bai J., Shih K., Zeng E.Y. & Cheng H., 2013. Assessing heavy metal pollution in the surface soils of a region that had undergone three decades of intense industrialization and urbanization. *Environmental Science and Pollution Research*, 20(9), 6150–6159. https://doi.org/10.1007/s11356-013-1668-z.

International Organization for Standardization, 2019. *Soil quality – Guideline for the screening of soil polluted with toxic elements using soil magnetometry* (ISO 21226:2019). https://www.iso.org/standard/70136.html [access: 13.11.2024].

Jabłońska M., Rachwał M., Wawer M., Kądziołka-Gaweł M., Teper E., Krzykawski T. & Smołka-Danielowska D., 2021. Mineralogical and chemical specificity of dusts originating from iron and non-ferrous metallurgy in the light of their magnetic susceptibility. *Minerals*, 11(2), 216. https://doi.org/10.3390/min11020216.

Kierczak J., Neel C., Aleksander-Kwaterczak U., Helios-Rybicka E., Bril H. & Puziewicz J., 2008. Solid speciation and mobility of potentially toxic elements from natural and contaminated soils: A combined approach. *Chemosphere*, 73(5), 776–784. https://doi.org/10.1016/j.chemosphere.2008.06.015.

Kondracki J., 2002. *Geografia regionalna Polski*. Wydawnictwo Naukowe PWN, Warszawa.

Kowalska J., Mazurek R., Gąsiorek M., Setlak M., Zaleski T. & Waroszewski J., 2016. Soil pollution indices conditioned by medieval metallurgical activity: A case study from Krakow (Poland). *Environmental Pollution*, 218, 1023–1036. https://doi.org/10.1016/j.envpol.2016.08.053.

Kowalska J.B., Mazurek R., Gąsiorek M. & Zaleski T., 2018. Pollution indices as useful tools for the comprehensive evaluation of the degree of soil contamination – A review. *Environmental Geochemistry and Health*, 40(6), 2395–2420. https://doi.org/10.1007/s10653-018-0106-z.

Lis J. & Pasieczna A., 1995. *Geochemical atlas of Poland: 1:2.500.000 = Atlas geochemiczny Polski*. Polish Geological Institute, Warsaw.

Magiera T., Strzyszcz Z., Kapička A. & Petrovský E., 2006. Discrimination of lithogenic and anthropogenic influences on topsoil magnetic susceptibility in Central Europe. *Geoderma*, 130(3–4), 299–311. https://doi.org/10.1016/j.geoderma.2005.02.002.

Magiera T., Jabłońska M., Strzyszcz Z., Rachwał M., 2011. Morphological and mineralogical forms of technogenic magnetic particles in industrial dusts. *Atmospheric Environment*, 45(25), 4281–4290. https://doi.org/10.1016/j.atmosenv.2011.04.076.

Magiera T., Łukasik A., Zawadzki J. & Roesler W., 2019. Magnetic susceptibility as indicator of anthropogenic disturbances in forest topsoil: A review of magnetic studies carried out in Central European forests. *Ecological Indicator*, 106, 105518. https://doi.org/10.1016/j.ecolind.2019.105518.

Magiera T., Kyzioł-Komosińska J., Dzieniszewska A., Wawer M. & Żogała B., 2020. Assessment of elements mobility in anthropogenic layer of historical wastes related to glass production in Izera Mountains (SW Poland). *Science of the Total Environment*, 735, 139526. https://doi.org/10.1016/j.scitotenv.2020.139526.

Magiera T., Górka-Kostrubiec B., Szumiata T. & Wawer M., 2021. Technogenic magnetic particles from steel metallurgy and iron mining in topsoil: Indicative characteristic by magnetic parameters and Mössbauer spectra. *Science of the Total Environment*, 775, 145605. https://doi.org/10.1016/j.scitotenv.2021.145605.

Magiera T. & Szuszkiewicz M., 2025. Combination of portable X-ray fluorescence with soil magnetometry as an effective tool for distinguish different pollution sources. *Land Degradation & Development*, 36(8), 2543–2556. https://doi.org/10.1002/ldr.5515.

Mazurek R., Kowalska J., Gąsiorek M., Zadrożny P., Józefowska A. & Zaleski T., 2017. Assessment of heavy metals contamination in surface layers of Roztocze National Park forest soils (SE Poland) by indices of pollution. *Chemosphere*, 168, 839–850. https://doi.org/10.1016/j.chemosphere.2016.10.126.

Mazurek R., Kowalska J.B., Gąsiorek M., Zadrożny P. & Wieczorek J., 2019. Pollution indices as comprehensive tools for evaluation of the accumulation and provenance of potentially toxic elements in soils in Ojców National Park. *Journal of Geochemical Exploration*, 201, 13–30. https://doi.org/10.1016/j.gexplo.2019.03.001.

Mossop K.F. & Davidson C.M., 2003. Comparison of original and modified BCR sequential extraction procedures for the fractionation of copper, iron, lead, manganese and zinc in soils and sediments. *Analytica Chimica Acta*, 478(1), 111–118. https://doi.org/10.1016/S0003-2670(02)01485-X.

Müller G., 1969. Index of geoaccumulation in sediments of the Rhine River. *GeoJournal*, 2, 108–118.

Podlešáková E., Němeček J. & Vácha R., 2001. Mobility and bioavailability of trace elements in soils. [in:] Iskandar I.K. & Kirkham M.B. (eds.), *Trace Elements in Soil: Bioavailability, Flux, and Transfer*, CRC Press, Boca Raton, 21–42.

Reimann C. & de Caritat P., 2005. Distinguishing between natural and anthropogenic sources for elements in the environment: regional geochemical surveys versus enrichment factors. *Science of the Total Environment*, 337(1–3), 91–107. https://doi.org/10.1016/j.scitotenv.2004.06.011.

Reimann C. & Garrett R.G., 2005. Background and threshold: critical comparison of methods of determination. *Science of the Total Environment*, 346(1–3), 12–27. https://doi.org/10.1016/j.scitotenv.2005.01.047.

Rozporządzenie, 2016. *Rozporządzenie Ministra Środowiska z dnia 1 września 2016 r. w sprawie sposobu prowadzenia oceny zanieczyszczenia powierzchni ziemi*. Dz.U. 2016 poz. 1395 [*Regulation of the Minister of the Environment of 1 September 2016 on the method of conducting the assessment of land surface contamination*. Journal of Laws of 2016 no. 2016, item 1395].

Różkowski J., Ślósarczyk K., Jakóbczyk-Karpierz S. & Rubin H., 2020. Występowanie i geneza WWA w wodach podziemnych obszaru Natura 2000 *Cieszyńskie Źródła Tufowe* oraz ochrona tych wód przed zanieczyszczeniem [Occurrence, sources of PAHs, and groundwater protection against pollution in the *Cieszyńskie Źródła Tufowe* Natura 2000 area]. *Przegląd Geologiczny*, 68(4), 249–255. https://doi.org/10.7306/2020.12.

Sajn R., 2005. Using attic dust and soil for the separation of anthropogenic and geogenic elemental distributions in an old metallurgic area (Celje, Slovenia). *Geochemistry: Exploration, Environment, Analysis*, 5(1), 59–67. https://doi.org/10.1144/1467-7873/03-050.

Szuszkiewicz M., Łukasik A., Magiera T. & Mendakiewicz M., 2016. Combination of geo- pedo- and technogenic magnetic and geochemical signals in soil profiles – Diversification and its interpretation: A new approach. *Environmental Pollution*, 214, 464–477. https://doi.org/10.1016/j.envpol.2016.04.044.

Szuszkiewicz M., Petrovský E., Łukasik A., Gruba P., Grison H. & Szuszkiewicz M.M., 2021. Technogenic contamination or geogenic enrichment in Regosols and Leptosols? Magnetic and geochemical imprints on topsoil horizons. *Geoderma*, 381, 114685. https://doi.org/10.1016/j.geoderma.2020.114685.

Wang X.S. & Qin Y., 2006. Use of multivariate statistical analysis to determine the relationship between the magnetic properties of urban topsoil and its metal, S, and Br content. *Environmental Geology*, 51(4), 509–551. https://doi.org/10.1007/s00254-006-0347-5.

Wawer M., 2020. Identification of technogenic magnetic particles and forms of occurrence of potentially toxic elements present in Fly ashes and soil. *Minerals*, 10(12), 1066. https://doi.org/10.3390/min10121066.

Zawadzki J., Szuszkiewicz M., Fabijańczyk P. & Magiera T., 2016. Geostatistical discrimination between different sources of soil pollutants using a magneto-geochemical data set. *Chemosphere*, 164, 668–676. https://doi.org/10.1016/j.chemosphere.2016.08.145.

Zhang C., Selinus O. & Kjellström G., 1999. Discrimination between natural background and anthropogenic pollution in environmental geochemistry – exemplified in an area of south-eastern Sweden. *Science of the Total Environment*, 243–244, 129–140. https://doi.org/10.1016/S0048-9697(99)00368-X.

Supplementary data associated with this article (Tables S1–S22) can be found in the online version at: https://doi.org/10.7494/geol.2025.51.2.133.